Automated detection and classification of hollow shapes in the Marburg University Forest.
A non-machine learning approach by means of multivariate statistical methods.

Schönberg Andreas B.Sc., Schwalb Jan B.Sc, Simon Christian B.Sc. & Agnes Schneider M.A.
M.Sc. students. Department of physical geography and environmental informatics.
Phillips University Marburg. Germany

Abstract
Automated detections of spatial objects plays a huge role in geomorphological and archaeological science. In this study we will use an automated segmentation algorithm to detect hollow shapes in the Marburg open forest (Mof) using only a LiDAR-based DEM. Further we will compute several artificial layers as predictor variables to classify the hollow shapes using hierarchic and kmeans clustering algorithms as a 'non machine learning' approach with multi-variant statistical methods.

1. Introduction

Automation has recently become a buzz-word in Sciences dealing with geographical data (OPITZ & HERRMANN, 2018; COWLEY 2012; BENNETT ET. AL. 2014). Despite the prejudice against automation (the human eye can see more freely and less restricted, every data is unique in it's own way) alone in Archaeology and Remote Sensing have seen hundreds of studies published between 2000 and 2015, dealing with automation (LAMBERS & TRAVIGLIA 2016, MAACK & PATERSON 2018). This methodological explosion has unfading relevance, because with the ever renewing data acquisition technologies our data is only becoming bigger and bigger day by day and we need methods which can deal with a huge amount of data.

The main directions of automation are today supervised and unsupervised (data extraction and analysis) in which machine learning or "classical" statistical methods can be applied. Moreover we can also distinguish between pixel- and object based image analysis (SEVERA ET. AL. 2016) which treats the (raster) data either on pixel or segment basis.

In our study we are using semi-automated segmentation to detect hollow shapes and classifiy craters, pingen and sinkholes in the Marburg Open Forest (MOF). Our hypothesis is, that we can automatically detect hollow shapes by segmentation on a sinks only model (SOM). Further we estimate that we can classify the hollow shapes by similarities using multivariate statistics (ordination and cluster analysis) on data of several artificially layers generated from a LiDAR-based DEM. In addition we generate ground truth and assume it to validate the results of our multi-variant statistical approach.

2. Methods

2.1 Remote Sensing Approach

2.1.1 Data Preprocessing

To generate data for the multivariate Statistic approach we need extracted pixel-values of different parameters for each hollow shape. To extract the values we first we need to detect and segment the hollow shapes and generate several artificially layers as parameters.

For the data preprocessing workflow (Fig.1) a DEM for the target area is generated from LiDAR data (Hessisches Landesamt 2007) with a resolution of 0.5 meters. Following we calculate a 'sinks only elevation model' (SOM) by subtracting a filled DEM from the DEM using the '*CENITH fillsinks'* function (SCHÖNBERG 2019). Further we perform a segmentation on the SOM using the '*CENITH hollow segmentation'* function (SCHÖNBERG 2019) to generate polygons representing the hollow shapes. The function requires parameters for the moving window and is able to erase

polygons by size of the area. To improve the results of the segmentation we created validation points (supervised hollow shape position) for each hollow shape and used the '*CENITH hollow validation'* function to get information about the hit-rate (correct detected), over- and under-segmentation and receive the best parameters for '*CENITH hollow segmentation'*. We set the minimum and maximum area size according to the typical area size of desired objects in the input DEM. In the next step we compute several artificial raster-layers from the DEM by using the '*LEGION dem'* function containing geomorphometrics (slope, aspect, curvature) and Skyview-factor (Visible Sky (svf) and related parameters) which are combined 17 layers.

Finally we extract the values from the artificial-layers for the polygons using the '*Reaver extraction'* function (SCHÖNBERG 2019). Because the ordination requires single values for each parameter the function calculates the standard deviation, mean, sum, minimum and maximum for every artificial layer per polygon resulting to 85 variables for each polygon.

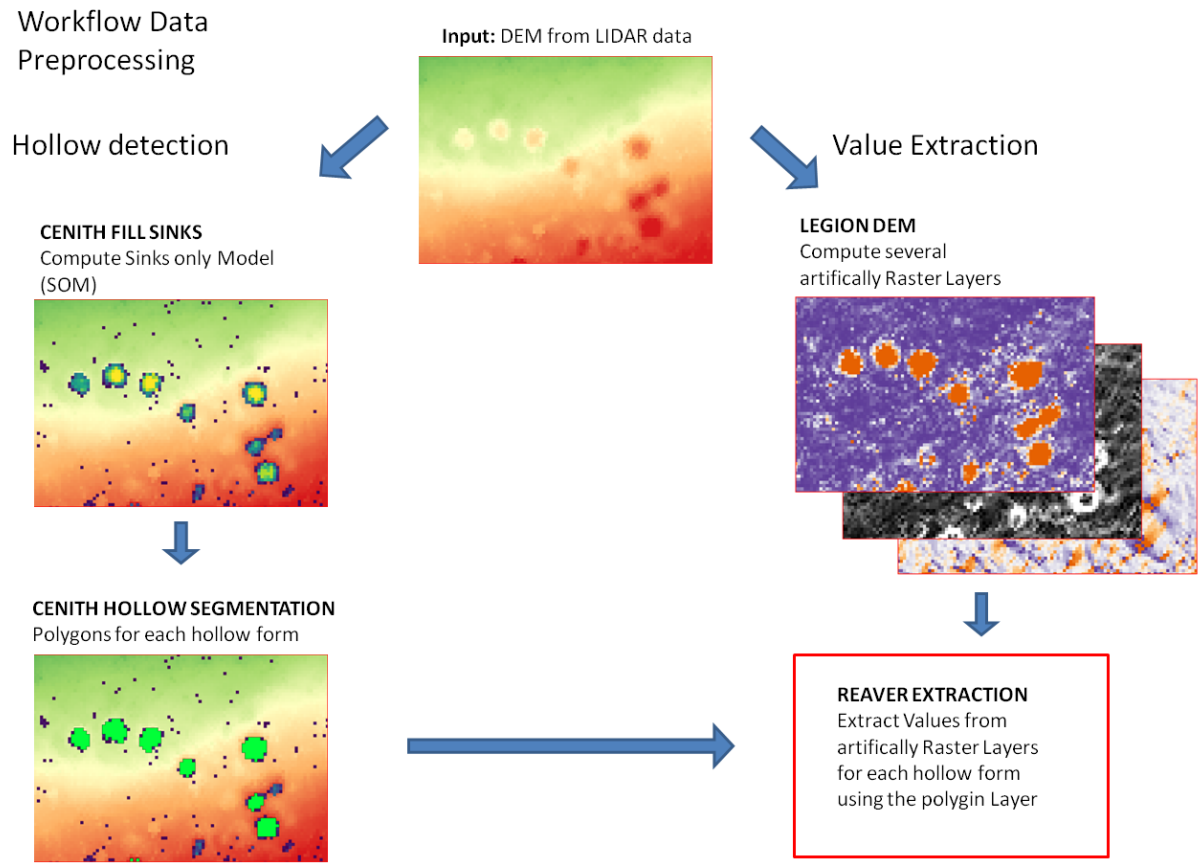

Fig. 1: *Remote sensing workflow "data preprocessing"*

2.1.2 Multi-Variant Statistical Approach

For the classification of hollow shapes by similarities we need training-datasets for each hollow shape class (crater, pingen and sinkholes) as well as test-datasets to verify the performance. Finally we need a dataset of the MOF for the prediction (Fig.2).

First we need areas where the hollow shape classes occur and can be separated to ensure that the extracted values represent the defined class. For the crater class we choose the Lahnberge because here we estimate hollow shapes to be explosion craters from the bombardment of the Marburg train-

station in World War Two. For sinkholes we choose an area in Bad Driburg due to the vast occurrence of limestone. To extract pingen we choose Neu Anspach where plenty well documented historic mining activities took place. The test-areas where selected near the training-areas for each class.

The areas of each class run through the data preprocessing to generate the datasets. In the following we perform an ordination and cluster-analysis using the '*Reaver hyperspace'* function SCHÖNBERG 2019) to assign the objects into three clusters using hierarchic clustering (HC) and K-means clustering. To further visualize the distances of the Objects the function computes a non-metric multi-dimensional scaling (nmds) and detrended correspondence analysis (dca) ordination. We estimate that the three classes are sorted in the three clusters due to similarities of the extracted values. To check the quality of the clusters we investigate how many objects of a single class are assigned to a cluster. When most objects of a class are assigned to one cluster we estimate it to be the classes representing cluster. We estimate that objects from other datasets (where the class is unknown) which are more similar to the objects of a representing cluster can be assumed as this class. For testing the cluster-quality we combined the training-dataset with each test-dataset and descriptively verified how well the known class of the test-dataset is assigned to the correct cluster.

Finally we generate a dataset for the area of interest (MOF) and perform '*Reaver hyperspace'* to predict the class of the hollow shapes detected in the area. Statements about the precision of the prediction are based on the test results.

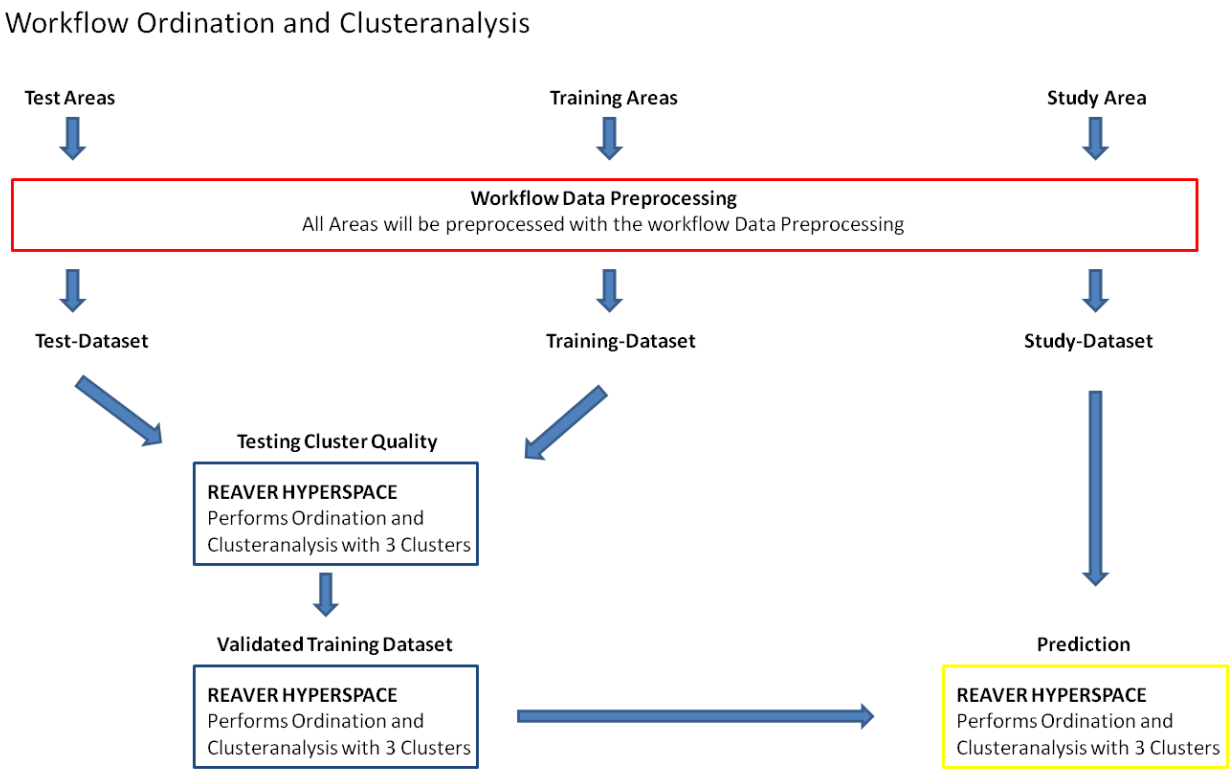

Fig. 2: *Workflow "ordination and cluster-analysis approach"*

2.2 Field Methods

To validate the outcome of the remote sensing approach, ground truth is required by field investigation. First it had to be understood how these hollow shapes can be described and what specific features and attributes have to be expected. According to these specific characteristics, the field methods have been chosen.

2.2.1 Distinction of Crater

This specific hollow shape is created by bomb detonation, which results in an artificially dense layer beneath, produced by high compression (NAGY 2015, AMBROSINI & LUCCIONI 2007, RAJU& GUDEHUS 1994). NAGY defines various crater-zones (Fig.3, after NAGY 2015, Fig.1.). The original crater boundary (1) is overlayed by a fall-back zone (2), which is consisted by the material which trickled back into the hollow shape after the explosion. Under the fall-back zone lies the rupture region (3), damaged by the explosion. The closing area of the hollow shape is the plastic zone (4), compressed by the detonation. This constitutes the most characteristic attribute of a bomb crater. Another descriptive feature is the ejecta (5), lumbing annularly around the hollow shape. Zone 2, 3 and 4 are missing under a pinge (depression resulting from mining) or sinkhole.

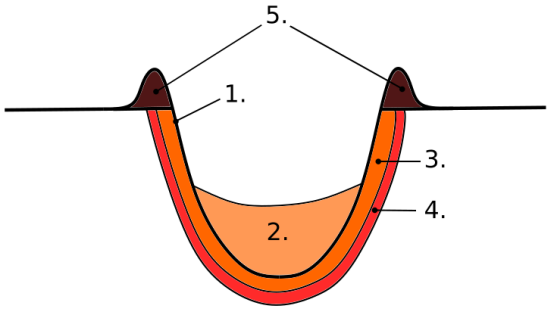

Fig. 3: The anatomy of a bomb crater.

2.2.2 Distinction of Pingen

Pingen are wedge-, ditch- or funnel-shaped depressions in the terrain caused by mining activity, which can be traced back even to neolithic times (HUSKE 2006). Their layout is caused by the collapse of an underground depletion or quarrying area, which is near to the surface (BISCHOFF & BRAMANN 1988). Pingen are extrinsicly hard to differentiate from bomb crater, because they can also depict an annular lumbing-area, as crater do. Furthermore, pingen can have steep or shallow embankment and their fill can be loose (ZEILER & GOLZE 2015, 368, ABB. 4.). On the other hand usually multiple pingen appear in a smaller area, sometimes even hundreds (KEMPA 2014, 212). What really differentiates pingen is, that anthropocentric traces can be found in their vicinity, like cart track or any traces of transportation from the pinge.

2.2.3 Distinction of Sinkholes (Doline)

Such as pingen, sinkholes are also depressions in the ground, caused by the collapse of the karstic surface layer. This said, sinkholes are the result of karst processes (ZEPP 2014), that is the solution of carbonate rocks or suffusion processes and appear only in karstic regions (LARD ET. AL. 1995). Sinkholes can be extremely variable in size, reaching from 1 to multiple hundred meters and also in form, being of natural origin. The lack of an annular lumb around the struture is a clearly distinguishing feature from crater and pingen. According to the geological map hollow shapes ID15 & ID19 are located in an area where slab-lime (Plattenkalk) is mapped. Therefore also sinkholes have been taken into consideration for possible hollow shapes in the MOF.

2.2.4 Used Field Methods

To manually classify hollow shapes in the field, two methods have been selected, which were found to be the most adapt to assess the geomorphological specificity of the outcome of the hollow detection (see 2.1.1) in the MOF).

The first method consisted of a 1 m core drill ("Pürckhauer") to produce core profiles. For the second method, a DPL-5 Dynamic Probe Light ("Künzelstab") was used to measure the density of the soil. Additionally general attributes (like shape or features) of the hollow shapes were described. In our FOI (Field of Interest) the geological map shows limestone for certain hollow shapes, so their substrate has been tested on chalk by a solution of 90 % water and 10 % hydrochloric acid.
The Dynamic Probe Light was chosen specifically for detecting the different horizons of crater. And the 1 m core drill allowed a more detailed examination of the underground in up to one meter depth.

Other methods (e.g. nivellement of the hollow shapes) have been excluded on the basis that geomorpholocial information of the hollow shapes like Slope, Aspect and Curvature were possible to extract from the DEM generated from the LiDAR data. Furthermore, pingen and sinkholes cannot be distinguished on the basis of the inclination of their embankment.

2.3 Workflow in the Field

Therefore, we set a catena of four profiles through the hollow shape (Fig.4). One, to get default values of the surrounding area, was taken some meters outside the hollow shape. The second one was taken on the rim of the structure, the third in the embankment (half way down) and the last one in lowest point of the hollow shape. In certain cases this workflow was adopted to the circumstances. On each profile, the DPL-5 and the core drill was used. Once in every hollow shape, the ground material was tested with HCl for existing limestone.

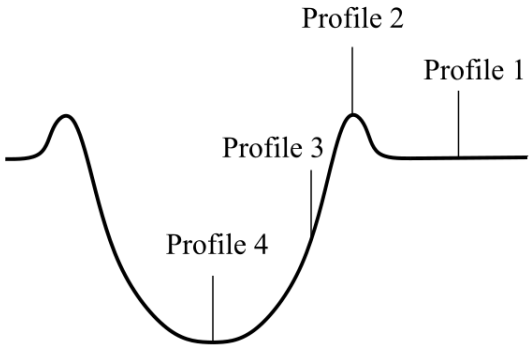

Fig. 4: Scheme of field workflow

3. Results

3.1 Remote Sensing

We hypnotized that we can detect hollow shapes by performing a segmentation on a SOM. With validation points and setting parameters for min and max area we reach 100% hit-rates for hollow shapes in each area with 'CENITH hollow segmentation'. Further we hypnotized that we can classify the hollow shapes by an ordination and cluster-analysis and assume that objects of the same class are assigned to a cluster by similarities.

For the training-dataset HC shows differentiated results (Fig.5) by assigning most craters in the first cluster, most pingen in the second cluster and all sinkholes in the third cluster. The K-means clustering does not return clear results. The craters and pingen are assigned together in one cluster while the sinkholes are devided into two cluster. For visualization the dca provides a clearer overview of the distances between the objects compared to the nmds. Therefore we use the results of the HC to evaluate the cluster quality.

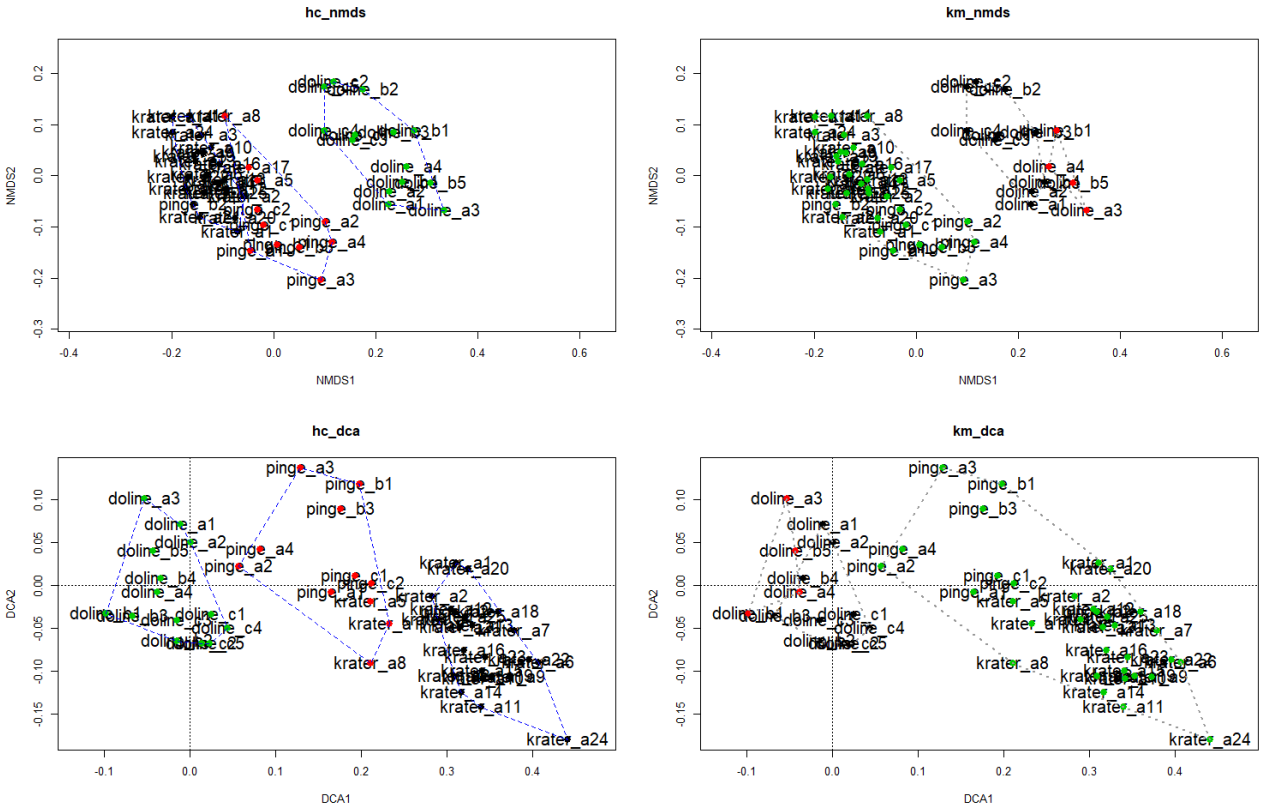

Fig. 5: *result HC and K-means clustering for training –dataset visualized with nmds and dca*

In the training-dataset 14/14 sinkholes are assigned to cluster 3 with no other class includes (Tab.1). Therefore we reach a 100% accuracy for sinkholes and assign cluster 3 as the sinkhole-cluster. Cluster 2 contains 8/9 pingen with 3/25 craters. We assume that cluster 2 represents the pingen-cluster with an accuracy of 88%. 22/25 crates are assigned to cluster 1 with 1/9 pingen. Therefore we assign cluster 1 as the crater-cluster with an accuracy of 88%. For the training-dataset we can prove our hypotheses.

To test our result we perform the multi-variant statistic approach tree times for each class using the training-data set combined with the respective test-dataset. The crater test-dataset is assigned to the crater-cluster with 11/14 objects (78 %) which is similar to the assignment of the training-dataset. Therefore we assume that we could prove that objects assigned to cluster 1 are craters with high probability. For the sinkhole test-dataset 3/14 objects (21%) are assigned to the sinkhole-cluster so that sinkholes cannot be predicted with high accuracy. With the pingen test-dataset we reach 6/14 objects to be assigned to the pingen-cluster with an accuracy of 42%. Based on this testing results we assume that our multi-variant statistical approach is able to detect craters properly but fails to predict the other two classes with high significance.

Area	HC cluster	Cluster class	Crater	C/n C	Pinge	P/n P	Sinkhole	S/n S	Class hit (%	Test objects	T/n T
Training	1	Crater	22/25	0.88	1/9	0.11	0/14	0.00	0.88	0/0	-
	2	Pinge	3/25	0.12	8/9	0.88	0/14	0.00	0.88	0/0	-
	3	Sinkhole	0/25	0.00	0/9	0.00	14/14	1.00	1.00	0/0	-
Test Craters	1	Crater	22/25	0.88	1/9	0.11	0/14	0.00	0.88	11/14	0.78
	2	Pinge	3/25	0.12	8/9	0.88	0/14	0.00	0.88	3/14	0.21
	3	Sinkhole	0/25	0.00	0/9	0.00	14/14	1.00	1.00	0/14	0.00
Test Sinkholes	1	Crater	22/25	0.88	1/9	0.11	0/14	0.00	0.88	1/14	0.07
	2	Pinge	3/25	0.12	8/9	0.88	0/14	0.00	0.88	10/14	0.71
	3	Sinkhole	0/25	0.00	0/9	0.00	14/14	1.00	1.00	3/14	0.21
Test Pingen	1	Crater	22/25	0.88	1/9	0.11	0/14	0.00	0.88	8/14	0.57
	2	Pinge	3/25	0.12	8/9	0.88	0/14	0.00	0.88	6/14	0.42
	3	Sinkhole	0/25	0.00	0/9	0.00	14/14	1.00	1.00	0/14	0.00
Study Area Mof	1	Crater	22/25	0.88	1/9	0.11	0/14	0.00	0.88	0/11	0.00
	2	Pinge	3/25	0.12	8/9	0.88	0/14	0.00	0.88	11/11	1.00
	3	Sinkhole	0/25	0.00	0/9	0.00	14/14	1.00	1.00	0/11	0.00

Tab. 1: Results of the assigned objects in clusters and cluster quality

Finally we use the validated training-dataset to predict the objects of the study area-dataset. We detected 11 hollow shapes in study area with most Objects within or near the boundaries of the MoF and one object in the far south east (ID 193) (Fig.6). Our multi-variant statistical approach shows that all hollow shapes (11/11) are assigned as pingen. With a view on the pingen test this result should be handled with caution.

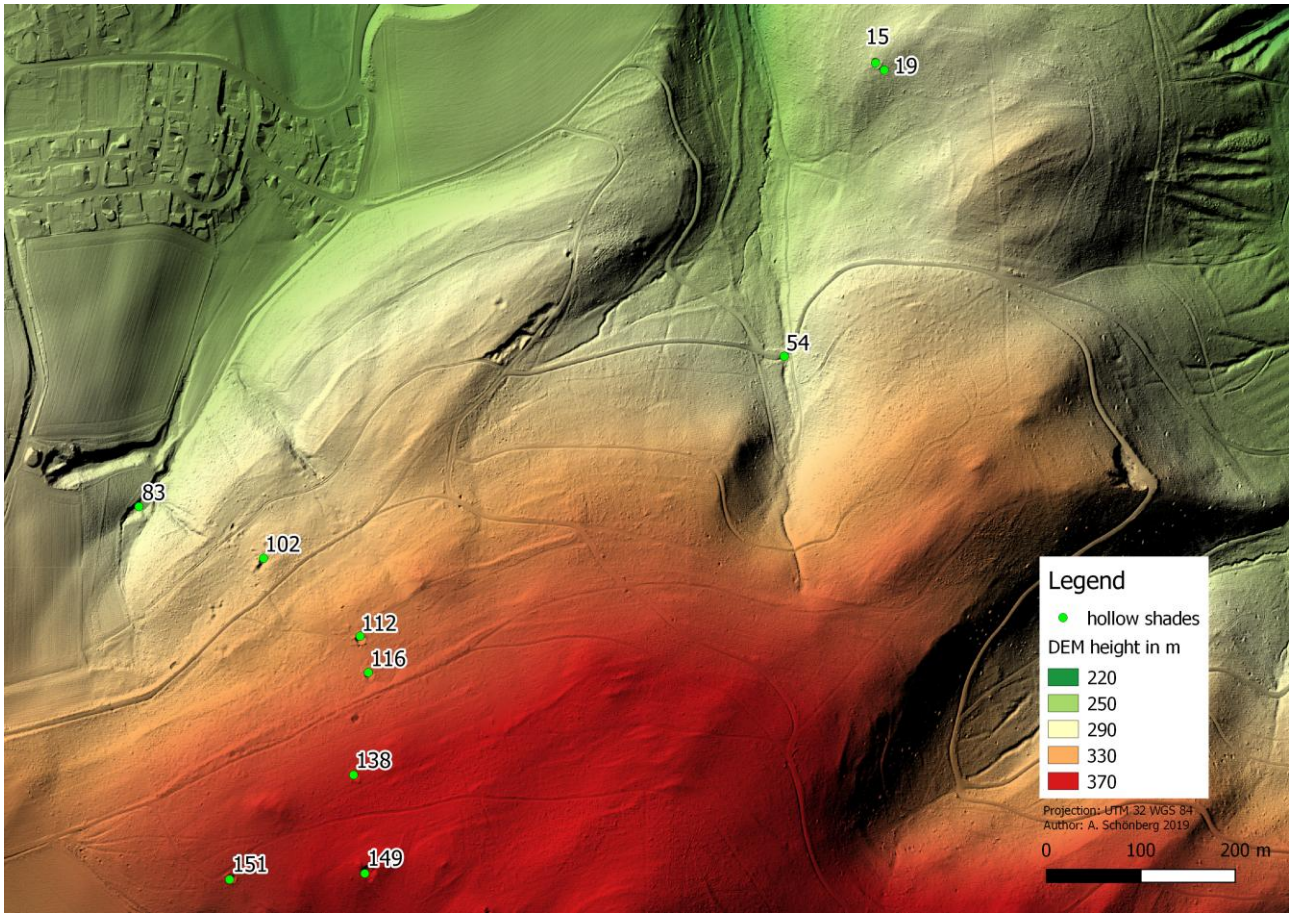

Fig. 6: Detected hollow shapes in the MoF. (ID 193 excluded for visualization purposes)

3.2 Fieldwork

In fieldwork, hollow forms with the ID's of 15, 19,112, 116, 138, 149 and 151 were examined. ID's 54 and 83 were dropouts and ID 102 was excluded because of time issues.
On the basis of the results of the DPL-5 and the 1 m core drill it was possible to identify 3 craters. As expected in most cases the 4th profile brought the best result regarding the structure of the hollow shapes. For our case study the supposed crater have been selected for discussion (**Fig.7**).
In the case of hollow shape ID 112.4 (meaning: ID 112, fourth profile) the plastic zone can be discerned very clearly around 60 to 70 cm depth. Hollow shape ID 116.4 shows two possible plastic zone areas, around 20 to 30 cm and 110 to 140 cm. ID 112 and ID 116 lie respectively next to each other, still they present different profiles. In case of ID 116 the question can be posed if the plastic zone is situated at already 20 to 30 cm or as we suppose in 110 to 140 cm depth and in the region between 20 to 30 cm the DPL-5 pushed through a stony area or a smaller stone and that is why the results are like this. ID 138 can be interpreted as crater structures, but the results are less clear as in the previous cases. ID 138.3 shows between 100 and 140 the supposed plastic zone.

ID 151 on the other hand can be excluded as crater, because there is no trace of an extensive and dense zone through the profiles (**Fig.8**). Additionally the annular lumb is incomplete. Thus we postulate that in this case we are dealing with a pinge. Because of harsh underground we were not able to use the core drill and the DPL-5 on ID 149. But a description of its general attributes points to a pinge.

As all examined hollow forms, the shapes with ID 15 & ID 19 have been tested with HCl because the geological map shows an occurrence of lime and has been found non-calcareous, thus there are no dolines in the MOF. A closer classification of this structures is not possible by our field results.

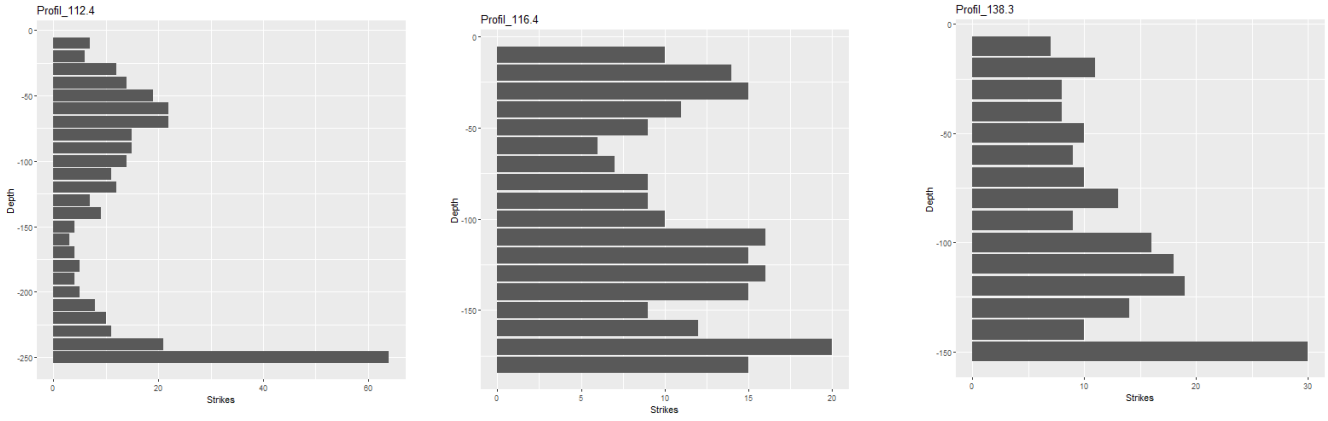

Fig. 7: DPL-5 profiles of the supposed crater

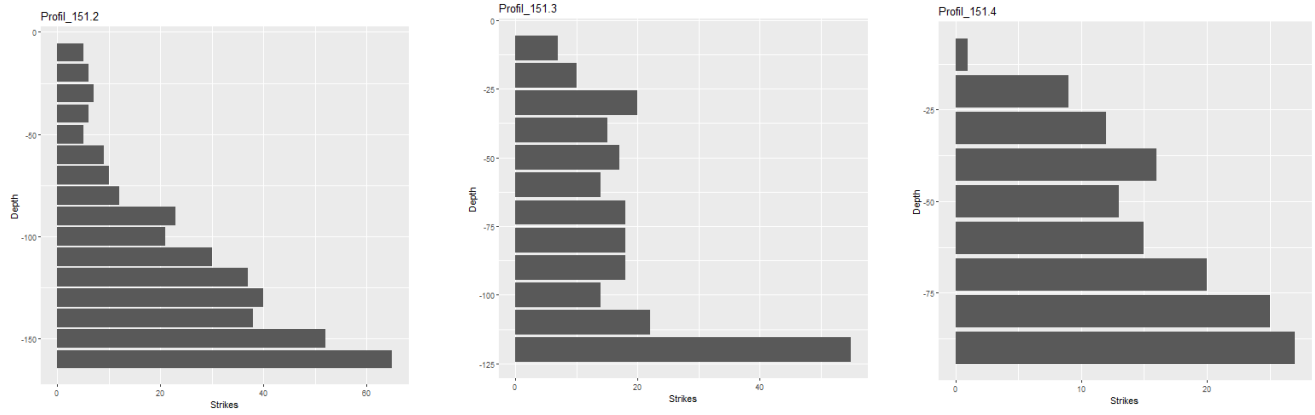

Fig. 8: DPL-5 profiles of the supposed sinkhole with ID 151

4. Discussion

4.1 Automation

The high accuracy of 100% for the segmentation of hollow shapes could be lead back to the fact that the SOM contains only raster cells within the sinks and small artifacts as well as huge structures are clipped by min and max area values. The main challenge is to get a preferably exact area to get representative values with the extraction.

For the training our main problem is that we don't have validated ground truth for the hollow shape classes in the extraction areas. We selected area where we know that there are respective objects of the classes but not which hollow shapes exactly. For example in an area with known craters due to World War 2 (Lahnberge) there could be pingen as well which we cannot keep apart. So maybe we assume pingen to be craters in our training data-set. This problem applies on all three classes.
Further while the form of craters is relatively similar to each other they can vary in radius (eg. craters from Tally bombs vs cluster bombs). With pingen they can vary in each from and size and can further vary much depending on the region. This problem can be also applied on the sinkhole with even more variations in size.
A reduction of input parameters could lead to an improvement in accuracy. In our approach we used all 85 variables (17 artificial rasters with 5 mathematic operations) with no filtering.

Nevertheless we get meaningful results for the training data and the crater test. The crater-dataset is extracted near the crater training-dataset. So we can assume a high similarity of the craters in the area. So maybe the less representative results for the pingen and sinkhole test-datasets results from varying object size and form. To improve the performance of our approach validated ground truth is recommended.

So we could prove our hypothesis that hollow shapes can be detected only based on a DEM and that we can classify craters with high accuracy while the prediction of pingen and sinkholes were not significant due to the cited problems above.

4.2 Field Method

On account of the field work it has been understood, that different crater zones (classification taken from NAGY 2014) appear in different depth of the structures, because these different zones have different dimensions, e.g. thickness, because of the topographic position of the hollow shapes. This means, that e.g. near to a summit the dimensions of the zones will be smaller.
Concerning the definition of the different hollow shapes in the accessible literature, these are often not clearly set. It is often assumed that the reader clearly knows how a certain hollow shape looks like, but if one would like to gather the scientific definition, attributes and specification of those structures, there is not much to find (exception are the crater). This makes it difficult to find appropriate field approaches which deliver clear data for the classification of hollow shapes.

The 1 m core drill proved not to be as effective as estimated. From the 24 drill profiles 63 horizons have been documented, 33 were empty. The present horizons were often only 2-3 cm thick in the drill. There was no drill profile which was complete. 8 drill profiles were completely empty.
In the case of the supposed craters (fall-back zone) it is understandable, but it is a phenomenon which occurred in all documented hollow shapes.
The DPL-5 was the method which delivered the best results, but in certain cases it was not applicable, e.g. in the case of ID 149, which was full of stones. Additionally in the summit area it was difficult to reach deeper, because the shallow soil thickness.

Finally we could not validate our multi-variant statistical approach with the ground truth. To much Object

5. Conclusions

The remote sensing approach results in the classification of 11 pingen. The fieldwork validation proved that three craters are within the study area. The other objects could not be assigned with certainty. Based on the given ground truth we are not able to validate the results of the multi-variant statistical approach.

Reviewing the cited problems we are able to automatically detect hollow shapes with a DEM which is usefull for several geomorphological and archeological questions. The main problems for the classification is the missing / inaccurate ground truth for training data. To improve the classification validated ground truth is highly recommended. Our own fieldwork methods did not provide clear results due to the cited distinguishing problems of hollow shapes.

Supporting Information

Additional field information
https://github.com/GeoMOER-Students-Space/Envimaster-Geomorph/tree/master/doc/Supporting%20information

Documentation for functions
https://github.com/GeoMOER-Students-Space/Envimaster-Geomorph/tree/master/src/docu_functions

6. References

AMBROSINI, D. & B. LUCCINOI (2007): Craters produced by explosionas above the soil surface. In: Elaskar, S. A., – Pilotta, E. A., – Torres, G. A., (Eds.) Mecánica Computactional, Vol XXVI, 2253-2266.

BENNETT R., COWLEY D., DE LAET V. (2014): The data explosion: tackling the taboo of automatic feature recognition in airborne survey data. Antiquity 88: 896–905. DOI: 10.1017/S0003598X00050766

BISCHOFF, W. & H. BRAMANN (1988): Westfälische Berggewerkschaftskasse Bochum. In: Das kleine Bergbaulexikon. Essen

COWLEY D, C. (2012): In with the new, out with the old? Auto-extraction for remote sensing archaeology. In: Bostater C.R, – Mertikas S.P., – Neyt X., – Nichol C., – Cowley D.C., – Bruyant, J.B., (Eds.) Remote Sensing of the Ocean, Sea Ice, Coastal Waters, and Large Water Regions 2012. Proceedings of SPIE 8532 Edinburgh: SPIE; 853206-1. DOI: 10.1117/12.981758

HUSKE, J. (2006): Die Steinkohlenzechen im Ruhrrevier. Deutsches Bergbaumuseum. Bochum

KEMPA, M. (2014): Albvorland-Eisenland. Mittelalterliche Eisenhütten zwischen Reutlingen und Nürtingen. Stuttart

LAMBERS, K. & A. TRAVIGLIA (2016): Automated detection in remote sensing archaeology: a reading list. AARGnews 53 (September 2016) 25-29. https://a-a-r-g.eu/ Publications tab

LARD, L., PAULL, C., HOBSON, B. (1995): "Genesis of a submarine sinkhole without subaerial exposure". Geology. 23, 10 (1995) 949–951.

MAACK, K. H. R. & D. PATERSON (2018): Systematic literature review on automated monument detection: A remote investigation on patterns within the field of automated monument detection. In:

NAGY, N. M. (2015): Numerical Evaluation of Craters Produced by Explosions on the soil Surface. Special Issue of the International Conference on Computational and Experimental Science and Engineeering (ICCESEN 2014). ACTA PHYSICA POLONICA A 128 (2015) 2-B, B260-B266.

OPITZ, R. & J. HERRMANN (2018): Recent Trends and Long-standing Problems in Archaeological Remote Sensing. Journal of Computer Applications in Archaeology, 1(1) 19–41, DOI: https://doi.org/10.5334/jcaa.11

RAJU, V.R. & G. GUDEHUS (1994): Compaction of loose sand depositsusing blasting. In: Proceeding of the 13th International Conference on Soil Mechanics and Foundation Engineering. New Delhi. 1994. 1145-1150.

Schönberg, A. (2019): CENITH, Reaver and LEGION functions. Marburg. Github: https://github.com/GeoMOER-Students-Space/Envimaster-Geomorph/tree/master/src

ZEPP, H. (2014): Geomorphologie. Eine Einführung. Grundriss Allgemeine Geographie. UTB Band 2164. Stuttgart

ZEILER, M. & R. GOLZE (2015): Montanarchäologische Untersuchungen an der Grube Gottessegen am Kindelsberg, Kreis Siegen-Wittgenstein. Ausgrabungen und Funde in Westfalen-Lippe 12(2015).https://www.academia.edu/22384357/Zeiler_and_Golze_2015_-_Montanarch%C3%A4ologische_Untersuchungen_an_der_Grube_Gottessegen_am_Kindelsberg_Kreis_Siegen-Wittgenstein_-_AFWL